Article

Structure

The Mechanism of ATP-Dependent Allosteric Protection of Akt Kinase Phosphorylation

Graphical Abstract

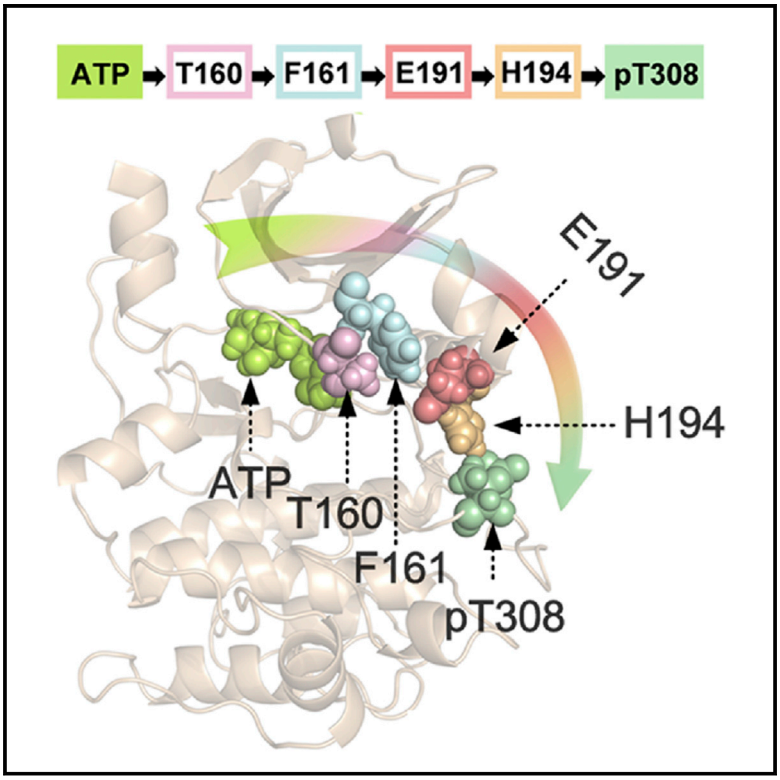

Authors

Shaoyong Lu, Rong Deng, Haiming Jiang, ..., Ruth Nussinov, Jianxiu Yu, Jian Zhang

Correspondence

jian.zhang@sjtu.edu.cn (J.Z.), jianxiu.yu@gmail.com (J.Y.)

In Brief

Lu et al. show that ATP, but not ADP, can protect Akt1 kinase phosphorylation through the allosteric pathway (ATP → T160 → F161 → E191 → H194 → pT308). This mechanism can provide a general model of allosteric kinase regulation by ATP. Furthermore, computation and experiments confirm that Akt1$^{H194R/R273H}$ double mutant is capable of rescuing pathology-related Akt1^{R273H}.

Highlights

- Kinases use ATP as source of phosphate groups to phosphorylate target substrates
- ATP can also allosterically regulate Akt1 kinase phosphorylation
- We propose a mechanism for allosteric regulation of Akt1 phosphorylation by ATP
- We identify a communication pathway from ATP to pT308 in Akt1 and its homologs

Lu et al., 2015, Structure *23*, 1725–1734
September 1, 2015
http://dx.doi.org/10.1016/j.str.2015.06.027

Structure
Article

The Mechanism of ATP-Dependent Allosteric Protection of Akt Kinase Phosphorylation

Shaoyong Lu,[1,5] Rong Deng,[2,5] Haiming Jiang,[1,5] Huili Song,[1,5] Shuai Li,[1] Qiancheng Shen,[1] Wenkang Huang,[1] Ruth Nussinov,[3,4,6] Jianxiu Yu,[2,6,*] and Jian Zhang[1,6,*]

[1]Department of Pathophysiology, Key Laboratory of Cell Differentiation and Apoptosis of Chinese Ministry of Education, Shanghai JiaoTong University, School of Medicine (SJTU-SM), Shanghai 200025, China

[2]Department of Biochemistry and Molecular Cell Biology & Shanghai Key Laboratory of Tumor Microenvironment and Inflammation, Shanghai JiaoTong University, School of Medicine (SJTU-SM), Shanghai 200025, China

[3]Cancer and Inflammation Program, Leidos Biomedical Research, Inc., Frederick National Laboratory, NCI, Frederick, MD 21702, USA

[4]Department of Human Genetics and Molecular Medicine, Sackler School of Medicine, Sackler Institute of Molecular Medicine, Tel Aviv University, Tel Aviv 69978, Israel

[5]Co-first author

[6]Co-senior author

*Correspondence: jian.zhang@sjtu.edu.cn (J.Z.), jianxiu.yu@gmail.com (J.Y.)

http://dx.doi.org/10.1016/j.str.2015.06.027

SUMMARY

Kinases use ATP to phosphorylate substrates; recent findings underscore the additional regulatory roles of ATP. Here, we propose a mechanism for allosteric regulation of Akt1 kinase phosphorylation by ATP. Our 4.7-μs molecular dynamics simulations of Akt1 and its mutants in the ATP/ADP bound/unbound states revealed that ATP occupancy of the ATP-binding site stabilizes the closed conformation, allosterically protecting pT308 by restraining phosphatase access and key interconnected residues on the ATP→pT308 allosteric pathway. Following ATP→ADP hydrolysis, pT308 is exposed and readily dephosphorylated. Site-directed mutagenesis validated these predictions and indicated that the mutations do not impair PDK1 and PP2A phosphatase recruitment. We further probed the function of residues around pT308 at the atomic level, and predicted and experimentally confirmed that Akt1$^{H194R/R273H}$ double mutant rescues pathology-related Akt1^{R273H}. Analysis of classical Akt homologs suggests that this mechanism can provide a general model of allosteric kinase regulation by ATP; as such, it offers a potential avenue for allosteric drug discovery.

INTRODUCTION

As a ubiquitously expressed serine/threonine protein kinase, Akt (also known as protein kinase B, or PKB) constitutes a central node in signaling cascades and plays a pivotal role as a signal transducer downstream of activated phosphoinositide 3-kinase (PI3K) (Franke et al., 1995; Vivanco and Sawyers, 2002). In mammalian cells, Akt is encoded by three highly homologous isoforms (sequence similarity >90%), designated as Akt1, Akt2 and Akt3, which are activated via a multi-step process. Akt activation is initiated by recruitment to the plasma membrane through the interaction of its pleckstrin homology (PH) domain with phosphatidylinositol-3,4,5-triphosphate (PIP_3), the product of PI3K generated upon insulin stimulation (Woodgett, 2005), or phosphatidylinositol-3,4-bisphosphate (PIP_2) (Dannemann et al., 2010). At the plasma membrane, T308 in the activation loop of the Akt1 kinase domain is phosphorylated by phosphoinositide-dependent kinase 1 (PDK1) (Manning and Cantley, 2007). Phosphorylation of the activation loop is critical for regulation of Akt activity. Phosphorylation of a second site at the C-terminal hydrophobic motif (S473) by mTORC2 (mammalian target of rapamycin complex 2) is required for maximal activation (Sarbassov et al., 2005). Dephosphorylation by protein phosphatase 2A (PP2A) abrogates Akt activity (Liao and Huang, 2010).

Activated Akt phosphorylates downstream targets to exert normal cellular functions, including cell survival, growth, proliferation, metabolism, migration, and angiogenesis (Cross et al., 1995; Datta et al., 1997). Consistent with its diverse roles, gain-of-function mutations are linked to cancer in humans, whereas loss-of-function mutations cause insulin resistance and diabetes (Manning and Cantley, 2007; Humphrey and James, 2013). Akt2-deficient mice eradicate insulin-dependent signaling in liver and skeletal muscle cells, deregulating glucose homeostasis, which results in insulin resistance (Cho et al., 2001). An inherited inactivating missense mutation R274H in the catalytic loop of the Akt2 kinase domain is linked to autosomal-dominant severe insulin resistance and diabetes mellitus in humans (George et al., 2004). Likewise, knockdown of PI3K-C2α expression and subsequent reduction of Akt1 activity in pancreatic β cells impairs glucose-stimulated insulin release (Leibiger et al., 2010). Since downregulating Akt is implicated in disease, many efforts have focused on uncovering Akt regulation and drug discovery (Arencibia et al., 2013).

Structurally, the architecture of the Akt kinase domain consists of two lobes (Figure 1): a smaller N-terminal lobe and a larger C-terminal lobe. ATP is bound in a deep cleft between them, located beneath a highly conserved glycine-rich nucleotide positioning motif, also called the G loop. In Akt1, the binding cleft of ATP locates approximately 20 Å from the phosphorylated T308 (pT308) in the activation loop, which is encapsulated by three

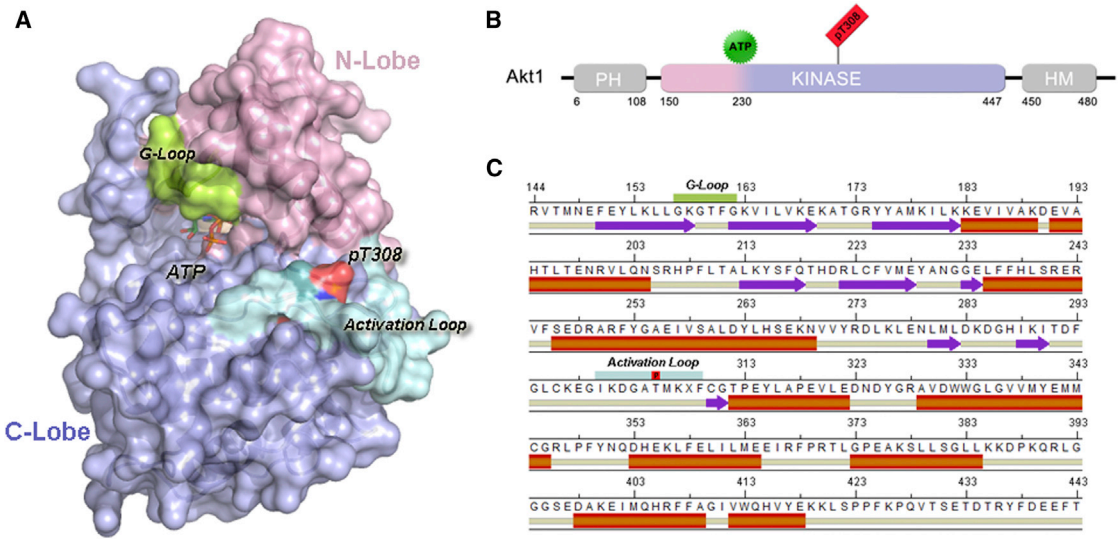

Figure 1. The Architecture of Akt1

(A) Surface representation of the activated Akt1 kinase domain (PDB: 4EKK) illustrating the surface locations of the N lobe (pink), G loop (green), activation loop (cyan), and C lobe (light blue). The locations of ATP in the ATP-binding site and pT308 in the activation loop are displayed.

(B) Domain structure of Akt1. The kinase domain is in the central region of the molecule. The pleckstrin homology (PH) domain acts as phosphoinositide-binding module, and the hydrophobic motif (HM) is located at the C terminus adjacent to the kinase domain.

(C) The Kabsch-Sander secondary structure cartoon of the Akt1 kinase domain. The purple solid arrows represent β strands, the red solid cylinders represent α helices, and the gray solid cylinders represent loops.

positively charged residues in the catalytic cleft: H194, R273, and K297. Phosphorylation of T308 acts as an "on" switch for Akt1 phosphorylation of its downstream substrates.

ATP occupancy of the ATP-binding cleft in Akt1 protects the pT308 level (Chan et al., 2011; Lin et al., 2012). Conversely, occupancy by ADP or the unbound state (*apo*) was markedly ineffective in maintaining the pT308 level. ATP-loaded pT308 resisted dephosphorylation by PP2A. This "on-off" switch model via ATP binding to Akt1 is important, since the universal function of ATP in protein kinases is to provide the γ-phosphate donor to phosphorylate substrates. In three-dimensional (3D) space, ATP is distant from pT308 with no direct interaction (Figure 1), suggesting allosteric communication from ATP in its binding cleft to pT308 in the catalytic cleft. However, the mechanism has been elusive.

Here, based on a total of 4.7-μs explicit solvent molecular dynamics (MD) simulations of Akt1 in the ATP/ADP bound/unbound states and its mutants, as well as experimental site-directed mutagenesis, we propose the molecular mechanism of ATP-dependent allosteric protection of pT308. Our results show that ATP binding allosterically protects the pT308 site by stabilizing the closed conformation of the Akt1 kinase domain, which can restrict phosphatase access. We observe that the allosteric pathway from ATP to the pT308 is connected by four residues, which is confirmed by site-directed mutagenesis. In contrast, in the ADP-bound or *apo* states, Akt1 is in its open conformation, which disrupts the allosteric, ATP-dependent protective pathway, thereby exposing pT308 from the catalytic cleft, making it accessible to phosphatase. Building on our resolved mechanism, we next explore the disease-related R273H mutation in the Akt1 kinase domain. Large-scale in silico screening of Akt1 mutants predicted that the H194R mutation can allosterically restore pT308 protection to the loss-of-function R273H mutant. The R273H/H194R double mutant was tested experimentally and observed to restore shielding of the phosphate moiety of pT308. Collectively, our data suggest a new model of Akt kinase regulation; together with the identified hotspots at the atomistic level along the ATP to pT308 allosteric pathway, it offers a path in therapy.

RESULTS

ATP Binding Protects the pT308 Site by Stabilizing the Closed Conformation of the Akt1 Kinase Domain, in Contrast to ADP Binding or the *Apo* Form

To identify the determinants of the molecular mechanism of Akt1 in the *apo*, ADP-bound, and ATP-bound states at the atomic level, a comparative analysis was first carried out using MD simulations (Bucher et al., 2011; Henzler-Wildman and Kern, 2007; Afanasyeva et al., 2014). To delineate Akt1 conformations in the different states, the probability distributions for two atom-pairs distances, one defined by the distance between the C_α atoms of H194 in helix C of the N lobe and pT308 in the activation loop of the C lobe (d_1), and the other between the C_α atoms of T160 in the tip of the G loop and G294 in the DFG loop (d_2), were calculated and converted into surface plots representing the energy landscapes (Text S1). Comparison of the energy landscapes of Akt1 in the different states indicated that the simulations were capable of capturing the population shifts between the *apo*, ADP-bound, and ATP-bound Akt1 (Figure S1). Cluster analysis (Text S1) of each MD trajectory further revealed that upon binding ATP, the N and C lobes of the Akt1 kinase domain were in a closed conformation, whereas in the ADP-bound or *apo* states the two lobes were in an open conformation (Figure 2). This difference was characterized by the distance between H194

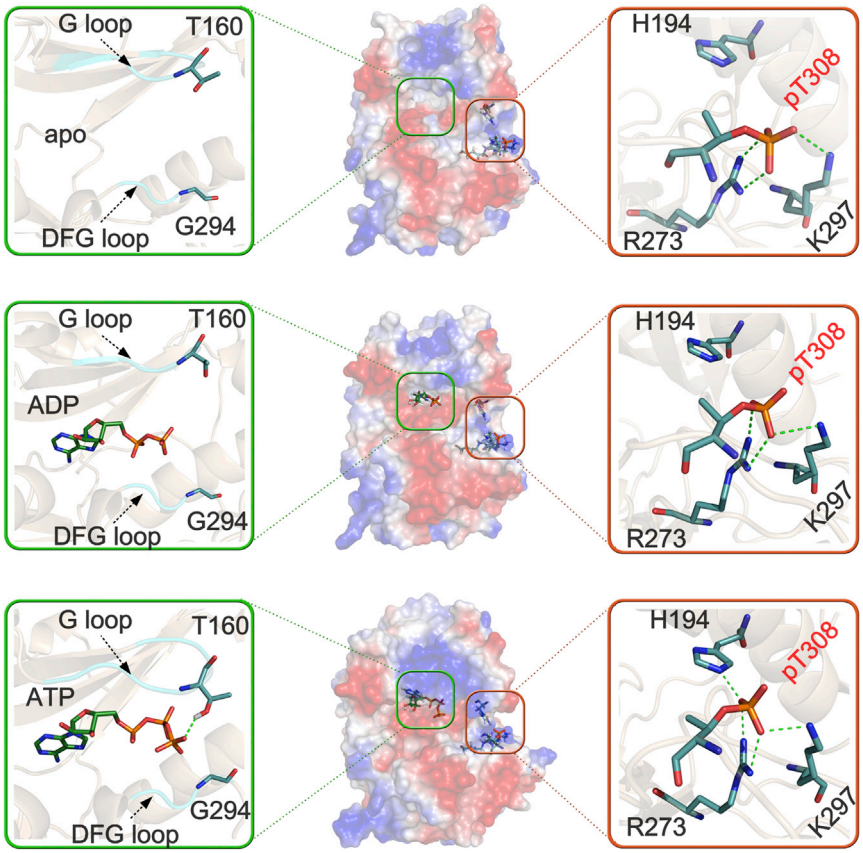

Figure 2. Conformational Analysis of Akt1 in the *apo*, ADP-Bound, and ATP-Bound States

The most representative structure for Akt1 in the *apo* (top), ADP-bound (middle), and ATP-bound (bottom) states obtained using cluster analysis from 200 ns of MD simulations. The surface of Akt1 is displayed by electrostatic potentials: positive charges are in blue, negative charges are in red, and neutral charges are in white. Details of interactions of ATP in the ATP-binding site and pT308 in the catalytic cleft for the three simulated systems are enlarged on the left- and right-hand side, respectively. The G and DFG loops are colored cyan, and salt bridges or H bonds are depicted by green dotted lines. See also Figures S1 and S2.

and pT308, which was 10.6 ± 0.4 Å in the ATP-bound state compared with 12.1 ± 0.6 Å in the ADP-bound state and 12.6 ± 1.0 Å in the *apo* state (Figure S2). In the ATP-binding cleft of the ATP-bound Akt1 (Figure 2, bottom), the hydroxyl group side chain of T160 formed a hydrogen bond (H bond) with the γ-phosphate moiety of ATP. Concomitantly, the phosphate moiety of pT308 in the activation loop was surrounded by the catalytic cleft residues H194, R273, and K297. In contrast, in the ADP-bound (Figure 2, middle) or *apo* states (Figure 2, top), the H bond between T160 and ADP was lost, accompanied by exposure of the phosphate moiety of pT308 from the catalytic cleft. These data suggest that ATP occupancy of its binding cleft stabilizes the closed conformational state of the Akt1 kinase domain, and shields pT308 in the catalytic cleft against phosphatase attack. Conversely, the open conformational state of Akt1 kinase domain in the ADP-bound or *apo* states could render the pT308 accessible to dephosphorylation.

To further determine the role of the closed conformation of Akt1 kinase domain in the ATP-dependent protection of pT308, we analyzed the trajectory of the wild-type (WT) ATP-bound Akt1 kinase domain and found that two pairs of salt bridges, K179···E198 and R200···E298, were maintained with >80% occupancy between the N and C lobes of Akt1. MD simulations of three ATP-bound Akt1 mutants, E198A, R200A, and E298A, were further performed to explore the effects of these mutations on the conformations of Akt1 (K179 was not mutated due to its interaction with the ATP α/β-phosphate moieties; mutating K179 would affect ATP binding). All mutations increased the distance between H194 and pT308 by approximately 12% compared with the WT. The solvent-accessible surface area (SASA) of pT308 in the E198A, R200A, and E298A mutants increased by approximately 28%, 42%, and 25%, respectively, compared with the WT. These data suggested that in all three mutants the two lobes of the kinase domain were in open conformation, with the pT308 phosphate moiety at the catalytic cleft exposed, which may enable pT308 dephosphorylation by phosphatases. The simulations further indicated that the closed conformation of the kinase domain tethered by these electrostatic interactions could be instrumental in the ATP-dependent protection of pT308. To validate this model, the three mutants were constructed in HeLa cells and tested for pT308 levels. As shown in Figure 3A, these mutants prominently diminished the pT308 levels compared with WT Akt1. Collectively, these results suggested that formation of the closed conformation of the Akt1 kinase domain is a prerequisite for ATP to exert allosteric protection of the pT308 site.

The Molecular Basis of the Allosteric Communication from ATP to pT308

ATP is ~20 Å away from pT308, and no direct interactions exist between them (Figure 1). To uncover the mechanism of signal propagation, we sought to identify residues in the allosteric communication from ATP in the ATP-binding cleft to pT308 in the catalytic cleft. The allosteric communication in the ATP-bound Akt1 was explored via our in-house method (Text S1) based on the Markov propagation analysis method developed by Chennubhotla and Bahar (2006) and the *NetworkView* method (Text S1) developed by Eargle and Luthey-Schulten (2012). Using the two methods, the optimal allosteric pathway from ATP to pT308 was identified as follows (Text S1; Figure S3)

$$\text{ATP} \rightarrow \text{T160} \rightarrow \text{F161} \rightarrow \text{E191} \rightarrow \text{H194} \rightarrow \text{pT308}.$$

Four residues located in the G loop (T160 and F161) and helix αC (E191 and H194) were found to be involved in propagating the

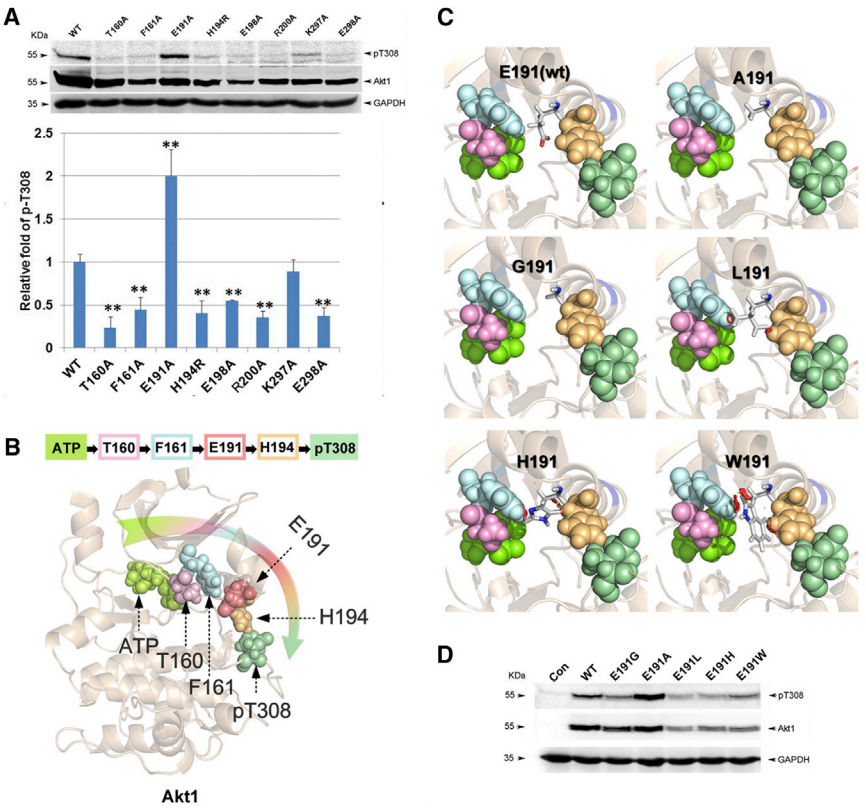

Figure 3. ATP-Dependent Allosteric Communication from ATP to pT308

(A) Effects of T160A, F161A, E191A, H194R, E198A, R200A, K297A, and E298A mutants on phosphorylated Akt1. MyrAkt1 (myristoylated Akt1) and Akt1 mutants were transfected into HeLa cells. After 48 hr, cells were lysed for western blots. MyrAkt1, pT308-MyrAkt1, and GAPDH were analyzed by immunoblotting (upper panel). An unpaired (equal variance) t test was performed on the relative levels of pT308 in each MyrAkt1 mutant compared with that of MyrAkt1 wild-type (WT) (lower panel) ($n = 3$; $^{**}p < 0.01$).

(B) The signal propagation pathway from ATP to pT308 in the ATP-bound Akt1.

(C) Schematic representation of the interactions of residue 191 with F161 and H194 in the WT, E191A, E191G, E191L, E191H, and E191W mutants. The generated steric hindrances in the E191L, E191H, and E191W mutants are colored red.

(D) Effects of E191G, E191A, E191L, E191H, and E191W mutants on phosphorylated Akt1. MyrAkt1 and mutants in both (A) and (D) were transfected into HeLa cells for 48 hr followed by immunoblot analysis of Akt1 T308 phosphorylation and HA-tagged MyrAkt1 expression.

See also Figures S3–S5.

signal from ATP to pT308 (Figure 3B). Alteration of the residues could then interrupt the propagation. Indeed, the H194A mutant abolishes ATP-dependent resistance to dephosphorylation (Chan et al., 2011). Inspired by this finding, we investigated the effects of T160, F161, and E191 on the allosteric pathway by mutagenesis in HeLa cells. As shown in Figure 3A, the T160A and F161A mutants reduced the pT308 level compared with WT Akt1, indicative of their involvements in the allosteric communication. Surprisingly, the E191A mutant showed a 2-fold increase of the pT308 level compared with WT Akt1. To unveil the unexpected change the conformational effect of E191 in the allosteric pathway was analyzed, and the result showed that the side-chain carboxyl group of E191 was H-bonded to the imidazole ring of H194, which, in turn, donated an H bond to the phosphate moiety of pT308 (Figure 3B). Presumably, the H bond from E191 draws H194 to weaken the protection of pT308 by H194, which can promote the likelihood of phosphatase access. When E191 is mutated to alanine, A191 is compatible with the cavity formed by F161 and H194 (Figure 3C) but the mutual attraction between A191 and H194 decreases, and the interaction between H194 and pT308 strengthens. The conformational difference (Valley et al., 2012) is supported by the energy change of H194···pT308 calculated by the two-layer ONIOM-based quantum mechanical/molecular mechanical method, with the interaction energy in the E191A mutant approximately −3.2 kcal/mol lower than in the WT (Text S2). Taken together, these data suggest that phosphatase resistance can be sufficient in the E191A mutant, more so than in the WT Akt1.

To further investigate the role of residue 191 side chain in the allosteric pathway from ATP to pT308, four additional mutants, E191G, E191L, E191H, and E191W, were constructed and tested. In the allosteric modeling, the lack of side chain in the E191G mutant abrogates the allosteric signal propagation from F161 to H194 (Figure 3C); larger volumes of side chains such as L191, H191, and W191 are not compatible with the cavity formed by F161 and H194 due to steric hindrance (Figure 3C). As expected, the E191G mutant showed a significant decrease in the pT308 level compared with WT Akt1 in our experimental test (Figure 3D), which is in good agreement with the theoretical model of allosteric communication from F161 to H194. In addition, protein expression of E191L, E191H, and E191W mutants was significantly reduced, and these effects are likely derived from structural instability due to steric conflicts. Thus, the combination of theoretical and experimental data lends support to the allosteric pathway from ATP to pT308, linking ATP binding and pT308 protection.

Akt1 is a multi-domain kinase consisting of PH, kinase, and hydrophobic motif (HM) domains (Wu et al., 2010). We observed that the allosteric protection pathway is in the Akt1 kinase domain (residues 144–443). To evaluate the pathway, we expressed, purified, and investigated the activated WT human Akt1(144–443) and its four mutants (T160A, F161A, E191A, and H194R), which we observed to be involved in the allosteric pathway in vitro (Wu et al., 2010; Kumar et al., 2001). We explored how the four mutations affected the dephosphorylation of pT308 by PP2A. The results showed that in the presence of ATP-γ-S, T160A/F161A/H194R mutants reduced the pT308 level compared with WT Akt1(144–443) while the E191A mutant effectively increased the resistance to T308 dephosphorylation (Figure S4), which is in good agreement with our full-length Akt1 results in HeLa cells (Figure 3A), suggesting that the identified allosteric pathway plays a protective role in the independent kinase domain.

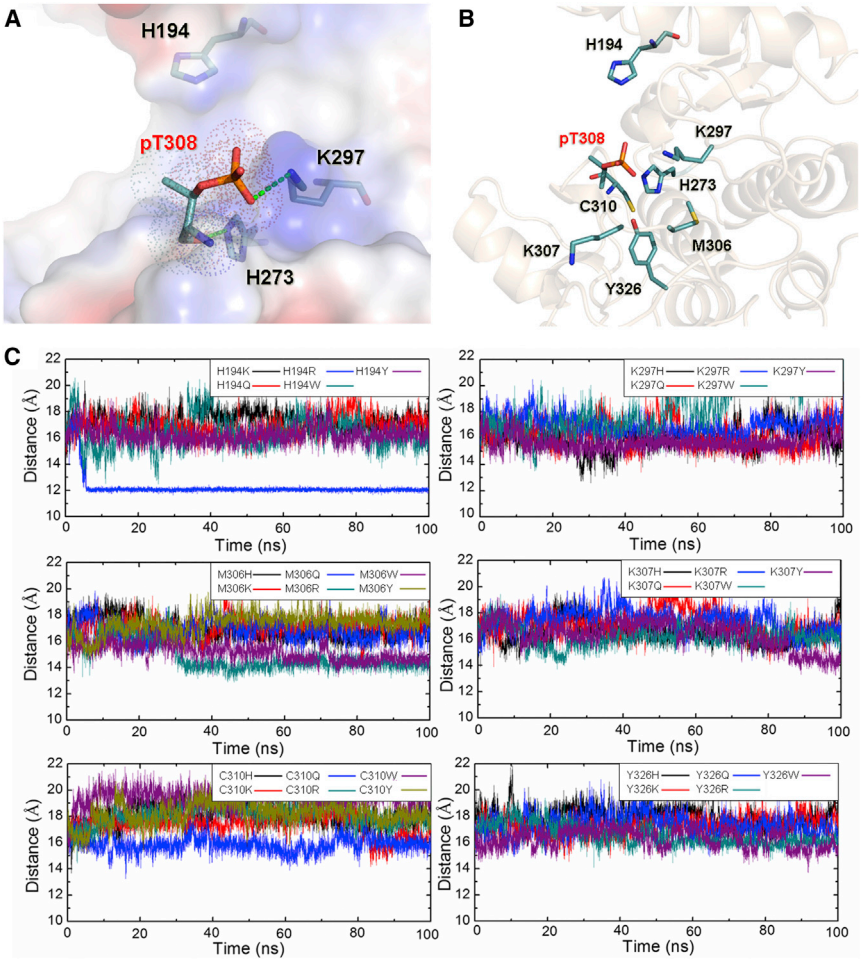

Figure 4. Design of a Rescue Protection of pT308 in the Akt1 R273H Mutant

(A) Details of the intramolecular interactions of pT308 with three residues in the catalytic cleft (H194, H273, and K297) of the Akt1 R273H mutant from 200 ns of MD simulation. The surface of pT308 is depicted by dots, and green dotted lines represent salt bridges or H bonds.

(B) Nearby residues including H194, K297, M306, K307, C310, and Y326 within a radius of 6 Å around pT308 are displayed in the Akt1 R273H mutant.

(C) In silico mutagenesis analysis of pT308-adjoining residues based on the Akt1 R273H mutant. For each mutant, MD simulation was carried out for 100 ns. The distances between the two C_α atoms of residues in positions 194 and 308 were measured in each mutant.

The Inability of the Akt1 R273H Mutant to Protect the pT308 Site

ATP binding allosterically promotes the burial of the phosphate moiety of pT308 in the catalytic cleft of Akt1 surrounded by H194, R273, and K297, which can restrict phosphatase access. These three residues can play a direct role in the protection of pT308. In addition to the established effects of H194 and R273, whose alanine mutants abolished the ATP-dependent phosphatase resistance (Chan et al., 2011), we explored the impact of K297 on the pT308 level. The results demonstrated that the K297A mutant had only a slight effect (Figure 3A). This indicated that both H194 and R273 act as dominant residues in the catalytic cleft. Remarkably, a highly homologous R274H in Akt2 (corresponding to R273 in Akt1) reported from diabetes patients is an ATP-dependent phosphatase-resistant loss-of-function mutant (George et al., 2004), similar to the Akt1 R273H mutant observed here (Figure 5A). Conformational analysis of the MD trajectories indicated that the pT308 phosphate moiety lost salt bridges/H bonds with residues 194 and 273 (from 100% to 0%) when R273 was replaced by H273, and was exposed from the catalytic cleft throughout the MD trajectory (Figure 4A). This persistent exposure of pT308 may cause its enhanced dephosphorylation by the phosphatase in the pathology-related mutant.

Akt1 H194R/R273H Double Mutant Restores pT308 Site Protection

The results reported above revealed that exposed pT308 failed to resist dephosphorylation by phosphatase in the pathology-related mutant, unlike in the embedded protective state. To confirm the hypothesis, we designed a rescue strategy for pT308 in the Akt1 R273H mutant by enhancing the interactions between other residues and pT308. First, most of the residues in the vicinity of pT308 including H194, K297, M306, K307, C310, and Y326 (Figure 4B) were respectively changed to H, K, Q, R, W, and Y based on the R273H mutant, yielding a total of 32 double mutants in silico (Table S1). Then 100-ns MD simulations were performed on each to investigate the effect of these substitutions on the protective ability of pT308. Among these putative double mutants, only the H194R mutation could decrease the distance between the N and C lobes (Figure 4C) and the SASA of pT308 from 63.8% to 24.1%, providing a significant potential recovery of the phosphatase resistance of pT308 of the double mutant. Finally, the pT308 level of H194R/R273H double mutant was obtained and compared with the WT Akt1. The results indicated that the double mutant restored the WT pT308 level (Figure 5A). To avoid some non-specific function by the additional H194R mutation, single H194R and double H194R/R273S mutants were tested. Both mutants were incapable of increasing the pT308 level in Akt1 on their own (Figure 5A), revealing the restoration by the additional H194R mutation in the R273H mutant.

To elucidate the reconstructed protection of pT308 in the H194R/R273H double mutant, the H194R/R273H MD simulation was extended to 200 ns and analyzed. As shown in Figure 5B, the phosphate moiety of pT308 formed two salt bridges with R194 and K297, and H273 formed an H bond with the backbone carbonyl group of pT308. These intramolecular interactions shielded the phosphate moiety of pT308 in the catalytic cleft, stabilized thereby the closed conformation of the kinase domain in the H194R/R273H double mutant, and rebuilt the allosteric

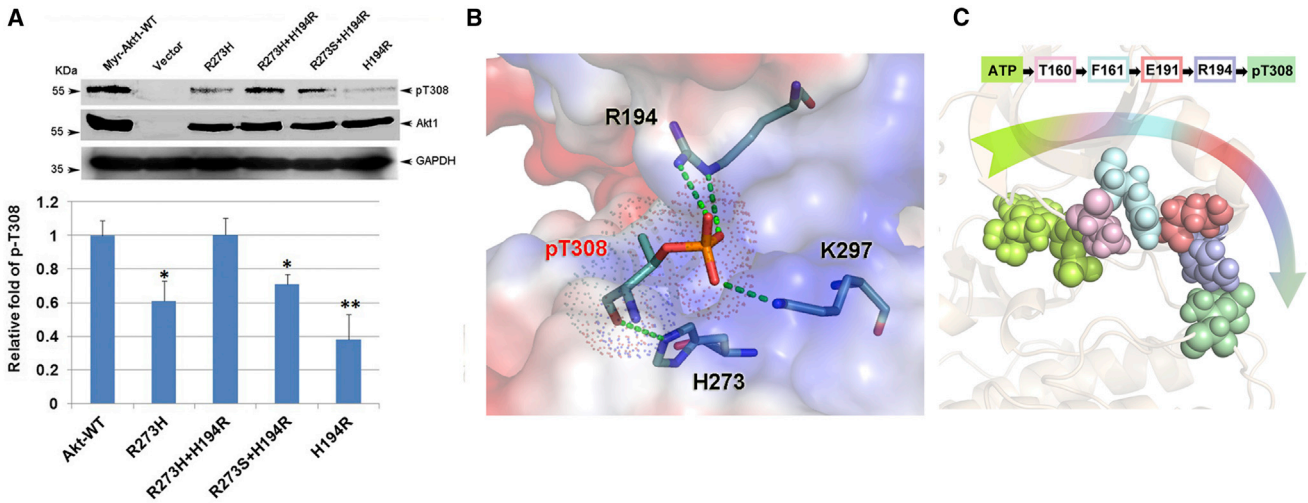

Figure 5. Akt1 H194R/R273H Double Mutant Restores Protection of pT308 against Dephosphorylation

(A) Effects of H194R and R273H single mutants as well as H194R/R273H and H194R/R273S double mutants on phosphorylated Akt1. MyrAkt1 and mutants were transfected into HeLa cells. After 48 hr, cells were lysed for western blots. MyrAkt1, pT308-MyrAkt1, and GAPDH were analyzed by immunoblotting (upper panel). An unpaired (equal variance) t test was performed on the relative levels of pT308 in each MyrAkt1 mutant compared with that of MyrAkt1-WT (lower panel) ($n = 3$; $^{*}p < 0.05$, $^{**}p < 0.01$).

(B) Details of the intramolecular interactions of pT308 with three residues in the catalytic cleft (R194, H273, and K297) of the Akt1 H194R/R273H double mutant from 200 ns of MD simulation. The surface of pT308 is depicted by dots, and green dotted lines represent salt bridges or H bonds.

(C) The signal propagation pathway from ATP to pT308 in the Akt1 H194R/R273H double mutant.

See also Figure S6.

communication from ATP to pT308 in the H194R/R273H double mutant (Figure 5C).

Mutations in Akt1 Do Not Impair Recruitment of PDK1 and PP2A

Akt is involved in the PI3K/Akt/mTOR pathway. Following growth factor stimulation, activated PI3Ks catalyze the conversion of PIP_2 to PIP_3, which directs the translocation of Akt to the plasma membrane (Woodgett, 2005; Manning and Cantley, 2007). At the membrane, T308 of Akt1 undergoes phosphorylation by PDK1. To test whether the mutations in the allosteric pathway impair the recruitment of PDK1 or phosphatase PP2A, the consequences of Akt1 mutations (T160A, F161A, E191A, H194R, and H194R/R273H) on pT308 levels were measured in the presence of the PP2A inhibitor Calyculin A and PDK1 inhibitor BX-795. The results showed that similar to changes in WT Akt1 (Figure 6A), pT308 levels in all mutants were markedly increased in the presence of Calyculin A, which was counteracted by co-treatment with BX-795 (Figure 6B). This result suggested that the mutations in Akt1 do not impair recruitment of PDK1 and PP2A.

DISCUSSION

ATP is generally used by protein kinases as the source of phosphate groups to phosphorylate their specific substrates. Recent evidence indicates that ATP can also function as an allosteric modulator (Huang et al., 2014; Lu et al., 2014a). Thus, understanding the allosteric mechanism of ATP in Akt1 may provide broader insights into the role of ATP and its mechanism as an endogenous modulator in cell signaling and in an important class of enzymes (Nussinov and Tsai, 2013; Lu et al., 2014b).

Communication between functional sites is central to protein regulation. In most cases, the pathways through which the signal propagates are poorly characterized (Goodey and Benkovic, 2008; del Sol et al., 2009; Lu et al., 2014c; Fetics et al., 2015). Here, we show that protection of pT308 level by ATP depends on formation of a finely tuned network of interactions within the G loop and helix αC. Network and mutational analyses identified four interconnected residues that directly communicate the ATP signal to the pT308. These data are in accordance with the notion that a small subset of physically connected residues propagates allosteric signals between distinct functional sites (Shen et al., 2011; Guo et al., 2015; Datta et al., 2008). To determine the specific pathway, we selected 12 additional residues in either the PH or kinase domains of Akt1, mutated them to alanine, and measured the pT308 levels of the mutants. These residues, located approximately 3–30 Å away from the allosteric pathway, were randomly selected on the surface of Akt1. As shown in Figure S5, the pT308 level of each mutant was almost the same as that of WT Akt1, indicating the specificity of residues in the identified allosteric pathway.

The molecular mechanism of Akt1 unraveled ATP-dependent allosteric signal propagation at the pT308 level, raising the possibility that allosteric communication could be a more general mechanism for regulation of phosphorylation in other kinases. To evaluate this possibility, several classical Akt1 kinase homologs (similarity >40%), including cAMP-dependent protein kinase (PKA) (Zheng et al., 1993), cyclin-dependent kinase 2 (CDK2), (Brown et al., 1999), TAO2 (Zhou et al., 2004), and PDK1 (Biondi et al., 2002), were selected to analyze the potential allosteric communication from ATP to the respective phosphorylation sites in the activation loop by multiple sequence

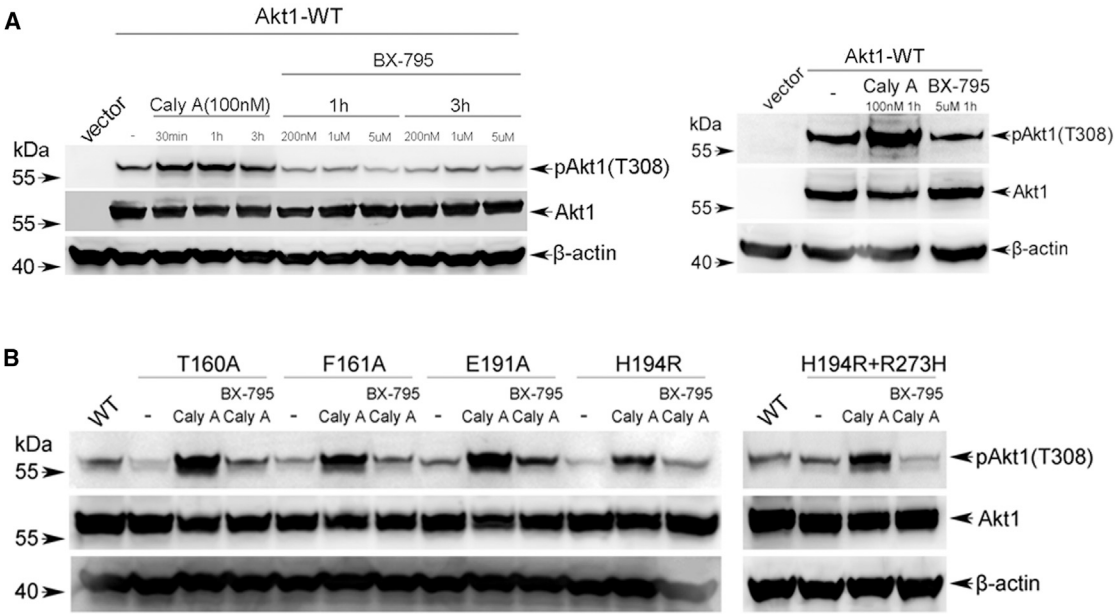

Figure 6. The Effect of MyrAkt1 Mutants in the Allsoteric Pathway for PDK1 and PP2A Recruitment

(A) Optimization of experimental conditions for two inhibitors in cells. HeLa cells were transfected with MyrAkt1-HA, and 48 hr after transfection the cells were treated with different concentrations of BX-795 and Calyculin A for different times, respectively. MyrAkt1 T308 phosphorylation, HA-tagged MyrAkt1, and β-actin were detected by immunoblotting.

(B) HeLa cells were transfected with MyrAkt1-HA mutants T160A, F161A, E191A, H194R, and H194R/R273H, and 48 hr after transfection cells were treated with 100 nM Calyculin A with or without 50 μM BX-795 for 1 hr. MyrAkt1 T308 phosphorylation (anti-pT308-Akt1), HA-tagged MyrAkt1 (anti-HA), and β-actin (anti-β-actin) expression were detected by immunoblotting.

alignment (Figure 7A). The results suggested that allosteric kinase regulation by ATP is conserved in these kinases (Figures 7B–7D). In addition, the protective effect of endogenous ligand binding has recently been described for a multi-subunit enzyme, AMP-activated protein kinase (Xiao et al., 2013). Taken together, in some kinases there is structural coupling between endogenous ligands and phosphorylation sites. Along similar lines, an "on-off" allosteric regulation by post-translational modifications is an established mode of regulation of dynamic signal transduction (Nussinov et al., 2012).

MD simulations and mutagenesis data revealed that Akt1 R273H mutation can result in dephosphorylation of pT308 by phosphatase, whereas the Akt1 H194R/R273H double mutant is able to rescue the pT308 level. These findings reflect the electrostatic potential of R194 in protecting pT308. Arginine is observed in corresponding positions in some homologous kinases such as CDK2 (Brown et al., 1999) and p38γ (Bellon et al., 1999). Crystal structures of CDK2 and p38γ demonstrate that in their phosphorylated states the arginine residue (R50 for CDK2 and R73 for p38γ) forms direct electrostatic interactions with the phosphorylated threonine of the two kinases, suggesting an active role for R194 in the protection of Akt1 phosphorylation. An opposite effect was observed for the WT and the R273H mutant in Akt1 (Figure 5A). Conformational analysis of the MD trajectory revealed that R194 in the Akt1 H194R mutant lost salt bridges with the phosphate moiety of pT308 due to spatial mismatch, resulting in pT308 exposure from the catalytic cleft throughout the H194R simulation (Figure S6), which could cause dephosphorylation of pT308 (Figure 5A). By contrast, in the H194R/R273H double mutant, R194 perfectly reconstructed the exquisite network of pT308 that shielded the phosphate moiety of pT308 (Figure 5). Collectively, these data suggest that both a positive electrostatic group and a structural match are important in the protection of pT308 in the Akt1 catalytic cleft. Recovery of phosphatase resistance of pT308 in the Akt1 R273H mutant by H194R could suggest new anti-diabetes strategies, or an allosteric drug mimicking this effect. Shearn et al. (2011) reported that modification of a crucial histidine by 4-hydroxy-2-nonenal in the catalytic cleft of Akt is able to inhibit insulin-dependent Akt signaling in HepG2 cells.

To conclude, our MD simulations of Akt1 in different states coupled with experiments unraveled the mechanism of allosteric regulation of Akt1 phosphorylation by ATP on the conformational level, and elucidated the function of a disease-related mutant and its rescue. Our analysis suggests that this regulation mechanism may hold for additional members of the Akt family. Finally, covalent modification of H194 in Akt1 R273H mutant may protect pT308, and constitute a covalent allosteric drug discovery rescue strategy for Akt2 R274H patients (Nussinov and Tsai, 2015).

EXPERIMENTAL PROCEDURES

Simulation Systems

The initial structure of Akt1 kinase domain in complex with the non-hydrolyzable ATP analog adenylyl imidodiphosphate (AMP-PNP), Mg^{2+}, and GSK3β-derived peptide was extracted from the PDB entry PDB: 4EKK (Lin et al., 2012). AMP-PNP was replaced by the physiological ATP to represent the ATP-bound Akt1 complex. The ADP-bound Akt1 complex was then

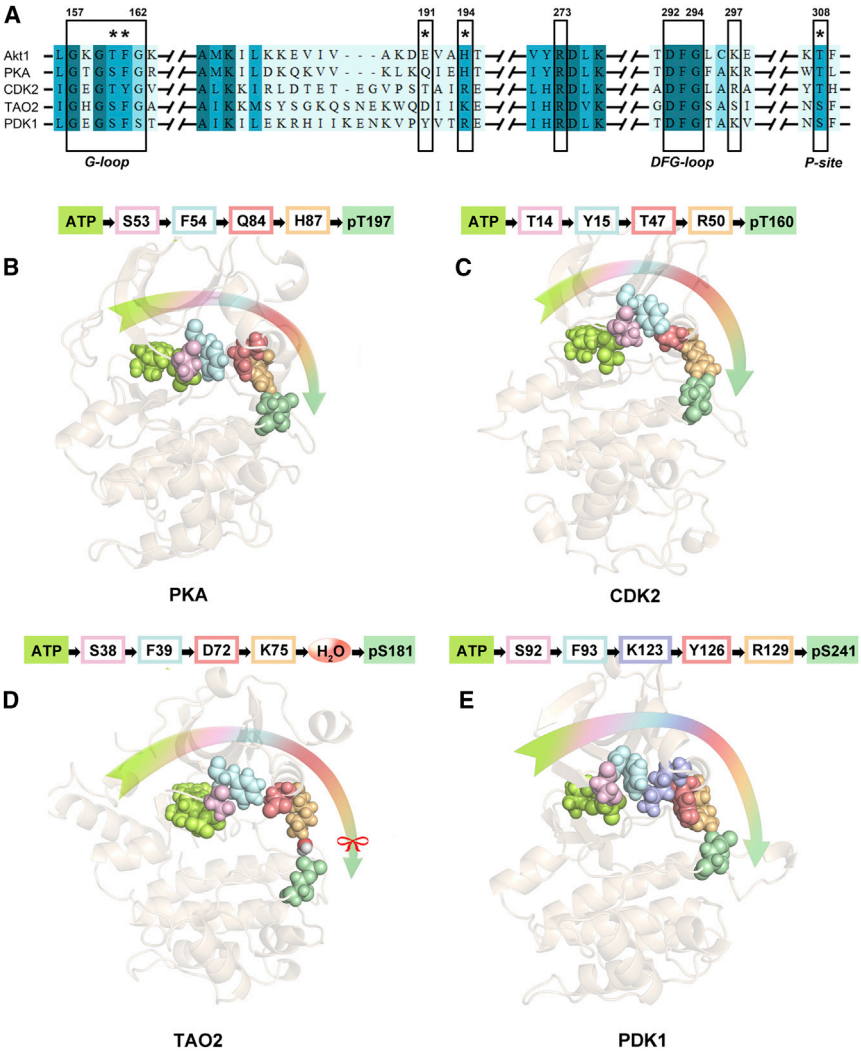

Figure 7. The Potential Allosteric Communication from ATP to the Respective Phosphorylation Sites in Other Kinases

(A) Multiple sequence alignment of the amino acids in the kinase domains of Akt1, PKA, CDK2, TAO2, and PDK1. This alignment was produced by the ClustalX2 program. Only representative sequences located in the allosteric pathway and in the catalytic cleft are shown. Residues in the allosteric pathway in this study are indicated by asterisks. The listed residue numbers refer to Akt1. Identical residues are marked dark cyan; similarity is indicated by light cyan.

(B) The signal propagation pathway from ATP to pT197 in PKA (PDB: 1ATP).

(C) The signal propagation pathway from ATP to pT160 in CDK2 (PDB: 1QMZ).

(D) The signal propagation pathway from ATP to pS181 in TAO2 (PDB: 1U5R).

(E) The signal propagation pathway from ATP to pS241 in PDK1 (PDB: 4AW0).

constructed by removing the γ-phosphoryl moiety of ATP, while the *apo* state was obtained by removing ATP from the active site. Akt1 mutants were constructed with the biopolymers module of SYBYL (Tripos Associates).

3D-RISM Calculation and Placevent Algorithm

The 3D reference interaction site model (3D-RISM) theory is an integral equation theory based on statistical mechanics (Imai et al., 2009), which generates accurate 3D solvent distribution function of water molecules around and inside a biomolecule of interest. The Placevent algorithm (Sindhikara et al., 2012) was then exploited to translate the continuous distributions from the 3D-RISM calculation to explicit water molecules. The detailed 3D-RISM calculation and Placevent algorithm are provided in Text S1. Based on the 3D-RISM and Placevent calculations, including the Placevent-predicted water molecules in the ATP-bound Akt1 complex is preferred (as compared with without Placevent-predicted water molecules) in reproducing the Akt1 active-site crystallographic architecture. Therefore, in the *apo*, ADP- and ATP-bound Akt1, as well as in all Akt1 mutants, we employed the corresponding initial models in complex with the Placevent-predicted water molecules for the MD simulations.

MD Simulations

MD simulations were performed with the AMBER 11 package (Case et al., 2005). Computation of the protonation state of titratable groups at pH 7.0 was carried out using the H^{++} web server (Gordon et al., 2005). The AMBER ff03 (Duan et al., 2003) force field was assigned for the protein. The parameters for ADP, ATP, and pT308 were taken from the AMBER parameter database. The starting protein complexes were explicitly solvated by TIP3P water molecules in the truncated octahedral box, where the distance to the edge of the solvent box from protein was set to be 10 Å. Counterions were added to maintain the electroneutrality of these systems. In total, 4.7-μs MD simulations of Akt1 in ATP/ADP bound/unbound and its mutants (Table S1) were performed. The detailed MD procedures are provided in Text S1.

Cell Culture, Plasmids, and Antibodies

HeLa cells were cultured in DMEM supplemented with 10% FBS, and 1% penicillin/streptomycin. Cells were maintained at 37°C under 5% CO_2. Myristoylated Akt1 from pCMV6-Myr-Akt1 was subcloned into the vector pEF-3HA to obtain the construct pEF-Myr-Akt1-HA (MyrAkt1) (Wang et al., 2000). All mutant constructs were generated by site-directed mutagenesis employing a PCR-based strategy according to the KOD-Plus-mutagenesis Kit protocol (Toyobo). Twenty-seven mutants (T160A, F161A, E191A, E191G, E191L, E191H, E191W, H194R, E198A, R200A, R273H, K297A, E298A, T101A, T105A, N199A, S216A, F236A, D262A, E278A, K301A, E355A, G373A, S381A, Y417A, R273H + H194R, R273S + H194R) were constructed, and the mutation sites and primers of Akt1 are listed in Table S2. Antibodies anti-Akt1 (2H10), anti-pT308-Akt1 (#9275), and anti-β-actin (13 × 10^5) were from Cell Signaling Technology; anti-PP2A-C (#05-421) was from Millipore; anti-His-tag (#66005-1-Ig) was from Proteintech; anti-GAPDH (glyceraldehyde-3-phosphate dehydrogenase) was from Sungene Biotechnology; and anti-HA-tag (16B12) was from Covance.

In-Culture Phosphorylated T308 Level of MyrAkt1 and Its Mutants

HeLa cells were transiently transfected with 4 μg of each plasmid (WT or mutated pEF-Myr-Akt1-HA) using Lipofectamine 2000 (Invitrogen) according to the manufacturer's protocols. After 48 hr, cells were lysed in SDS buffer (62.5 mM Tris-HCl, 2% SDS [pH 6.8]) and boiled for 10 min. Usually 200 μg of each lysate was subjected to 10% SDS-PAGE. For western blotting analysis, the primary antibodies anti-Akt1 (2H10), anti-pT308-Akt1 (Cell Signaling Technology), and anti-GAPDH (Sungene Biotechnology) were used at a 1:1,000 dilution in TBST buffer containing 5% BSA.

In-Culture Dephosphorylation of MyrAkt1 and Its Mutants

HeLa cells were transfected with plasmid of MyrAkt1 (or its mutants) as described above. After 48 hr of transfection, inhibitors (Calyculin A or Calyculin

A + BX-795) were added to medium and incubated at 37°C for 1 hr, then cells were lysed and dephosphorylation of MyrAkt1 (or its mutants) was analyzed by western blotting as previously described (Chan et al., 2011).

Expression and Purification of Akt1(144–443) Proteins

Human Akt1(144–443) protein and its four mutants T160A, F161A, E191A, and H194R were expressed in Sf9 cells (Invitrogen) with an N-terminal hexahistidine (His) tag, and purified in vitro using the general protocol described previously (Kumar et al., 2001; Wu et al., 2010). The proteins were enriched from the Sf9 cell lysate on Ni-NTA Agarose (Qiagen), then eluted from the Ni beads in a buffer consisting of 25 mM Tris-HCl (pH 8.0), 0.3 M NaCl, 0.05% (v/v) 2-mercaptoethanol, 100 mM imidazole, 10% (v/v) glycerol, and Complete EDTA-free protease inhibitor (Roche). The proteins were further purified via Superdex 200 size-exclusion chromatography (GE Health Biosciences) using the final storage buffer of 25 mM Tris-HCl (pH 7.5), 100 mM NaCl, 10% glycerol, and 5 mM DTT. All purification steps were performed at 4°C and the final proteins were stored at −80°C.

In Vitro Phosphorylation of Akt1(144–443) and Its Mutants

PDK1 (Active Motif) was used to phosphorylate Akt1(144–443) protein and its four mutants for activation in vitro according to the manufacturer's protocol. 14 μg of Akt1(144–443) protein (or each mutant) was added to a 50-μl solution of 50 mM Tris-HCl (pH 7.5), 0.1 mM EDTA, 2 mM DTT, 10 mM $MgCl_2$ containing 0.7 μg of PDK1, and 100 μM ATP (Sigma). The mixture was incubated for 30 min at 30°C and the remaining ATP in solution was removed using ProbeQuant G-50 Micro Columns (GE Healthcare) for further dephosphorylation assay.

In Vitro Dephosphorylation of Akt1(144–443) and Its Mutants by PP2A-C

Phosphorylated Akt1(144–443) protein and its four mutants were dephosphorylated in vitro by PP2A-C according to the manufacturer's protocol. To assess the effect of ATP-γ-S (Biolog) on the dephosphorylation, phosphorylated Akt1(144–443) protein (or each mutant) was aliquoted and pre-incubated with or without 500 μM ATP-γ-S for 10 min at 30°C in phosphatase assay buffer (50 mM HEPES [pH 7.5], 100 mM NaCl, 1 mM DTT, 10 mM $MgCl_2$), then 80 ng of PP2A-C was added and incubated for 50 min at 30°C in a final volume of 30 μl. Phosphatase reactions were terminated with SDS sample buffer, and Akt1 T308 phosphorylation (anti-pT308-Akt1), total His-Akt1 (144–443) (anti-His), and PP2A-C (anti-PP2A-C) were analyzed by immunoblots.

Statistical Analysis

Quantitation was analyzed by ImageJ v1.46 (NIH), and the relative intensity of the Akt1 pT308 band was normalized to the corresponding total Akt1. For all bar plots, the quantitative data were presented as means ± SD of three independent measurements. The statistical significance of compared measurements was evaluated using the two-tailed unpaired Student's t test, and a p value of <0.05 (*) or <0.01 (**) was considered statistically significant.

SUPPLEMENTAL INFORMATION

Supplemental Information includes two supplemental texts, six figures, and two tables and can be found with this article online at http://dx.doi.org/10.1016/j.str.2015.06.027.

AUTHOR CONTRIBUTIONS

S.L., R.N., J.Y., and J.Z. conceived and designed the study. S.L., Q.S., S.L., and W.H. performed computational studies. R.D., H.J., and H.S. performed experimental studies. S.L., R.N., J.Y., and J.Z. prepared and wrote the manuscript. All authors edited and approved the manuscript.

ACKNOWLEDGMENTS

This work was supported by the National Basic Research Program of China (973 Program) (2015CB910403); National Natural Science Foundation of China (81322046, 81302689, 81473137); Shanghai Rising-Star Program (13QA1402300); Program for New Century Excellent Talents in University (NCET-12-0355); and China Postdoctoral Science Foundation (2014M551426). This work has also been funded in whole or in part with Federal funds from the National Cancer Institute, NIH, under contract number HHSN261200800001E. This research was supported (in part) by the Intramural Research Program of the NIH, National Cancer Institute, Center for Cancer Research.

Received: January 11, 2015
Revised: May 11, 2015
Accepted: June 23, 2015
Published: August 6, 2015

REFERENCES

Afanasyeva, A., Hirtreiter, A., Schreiber, A., Grohmann, D., Pobegalov, G., McKay, A.R., Tsaneva, I., Petukhov, M., Käs, E., Grigoriev, M., and Werner, F. (2014). Lytic water dynamics reveal evolutionarily conserved mechanisms of ATP hydrolysis by TIP49 AAA+ ATPases. Structure *22*, 549–559.

Arencibia, J.M., Pastor-Flores, D., Bauer, A.F., Schulze, J.O., and Biondi, R.M. (2013). AGC protein kinases: from structural mechanism of regulation to allosteric drug development for the treatment of human diseases. Biochim. Biophys. Acta *1834*, 1302–1321.

Bellon, S., Fitzgibbon, M.J., Fox, T., Hsiao, H.-M., and Wilson, K.P. (1999). The structure of phosphorylated p38γ is monomeric and reveals a conserved activation-loop conformation. Structure *7*, 1057–1065.

Biondi, R.M., Komander, D., Thomas, C.C., Lizcano, J.M., Deak, M., Alessi, D.R., and van Aalten, D.M. (2002). High resolution crystal structure of the human PDK1 catalytic domain defines the regulatory phosphopeptide docking site. EMBO J. *21*, 4219–4228.

Brown, N.R., Noble, M.E.M., Endicott, J.A., and Johnson, L.N. (1999). The structural basis for specificity of substrate and recruitment peptides for cyclin-dependent kinases. Nat. Cell Biol. *1*, 438–443.

Bucher, D., Grant, B.J., Markwick, P.R., and McCammon, J.A. (2011). Accessing a hidden conformation of the maltose binding protein using accelerated molecular dynamics. PLoS Comput. Biol. *7*, e1002034.

Case, D.A., Cheatham, T.E., III, Darden, T., Gohlke, H., Luo, R., Merz, K.M., Jr., Onufriev, A., Simmerling, C., Wang, B., and Woods, R. (2005). The Amber biomolecular simulation programs. J. Comput. Chem. *26*, 1668–1688.

Chan, T.O., Zhang, J., Rodeck, U., Pascal, J.M., Armen, R.S., Spring, M., Dumitru, C.D., Myers, V., Li, X., Cheung, J.Y., and Feldman, A.M. (2011). Resistance of Akt kinases to dephosphorylation through ATP-dependent conformational plasticity. Proc. Natl. Acad. Sci. USA *108*, 1120–1127.

Chennubhotla, C., and Bahar, I. (2006). Markov propagation of allosteric effects in biomolecular systems: application to GroEL-GroES. Mol. Syst. Biol. *2*, 1–13.

Cho, H., Mu, J., Kim, J.K., Thorvaldsen, J.L., Chu, Q., Crenshaw, E.B., III, Kaestner, K.H., Bartolomei, M.S., Shulman, G.I., and Birnbaum, M.J. (2001). Insulin resistance and a diabetes mellitus-like syndrome in mice lacking the protein kinase Akt2 (PKBβ). Science *292*, 1728–1731.

Cross, D.A., Alessi, D.R., Cohen, P., Andjelkovich, M., and Hemmings, B.A. (1995). Inhibition of glycogen synthase kinase-3 by insulin mediated by protein kinase B. Nature *378*, 785–789.

Dannemann, N., Hart, J.R., Ueno, L., and Vogt, P.K. (2010). Phosphatidylinositol 4,5-bisphosphate-specific AKT1 is oncogenic. Int. J. Cancer *127*, 239–244.

Datta, S.R., Dudek, H., Tao, X., Masters, S., Fu, H., Gotoh, Y., and Greenberg, M.E. (1997). Akt phosphorylation of BAD couples survival signals to the cell-intrinsic death machinery. Cell *91*, 231–241.

Datta, D., Scheer, J.M., Romanowski, M.J., and Wells, J.A. (2008). An allosteric circuit in caspase-1. J. Mol. Biol. *381*, 1157–1167.

del Sol, A., Tsai, C.-J., Ma, B., and Nussinov, R. (2009). The origin of allosteric functional modulation: multiple pre-existing pathways. Structure *17*, 1042–1050.

Duan, Y., Wu, C., Chowdhury, S., Lee, M.C., Xiong, G., Zhang, W., Yang, R., Cieplak, P., Luo, R., Lee, T., et al. (2003). A point-charge force field for molecular mechanics simulations of proteins. J. Comput. Chem. *24*, 1999–2012.

Eargle, J., and Luthey-Schulten, Z. (2012). NetworkView: 3D display and analysis of protein·RNA interaction networks. Bioinformatics *28*, 3000–3001.

Fetics, S.K., Guterres, H., Kearney, B.M., Buhrman, G., Ma, B., Nussinov, R., and Mattos, C. (2015). Allosteric effects of the oncogenic RasQ61L mutant on Raf-RBD. Structure *23*, 505–516.

Franke, T.F., Yang, S.I., Chan, T.O., Datta, K., Kazlauskas, A., Morrison, D.K., Kaplan, D.R., and Tsichlis, P.N. (1995). The protein kinase encoded by the Akt protp-oncogene is a target of the PDGF-activated phosphatidylinositol 3-kinase. Cell *81*, 727–736.

George, S., Rochford, J.J., Wolfrum, C., Gray, S.L., Schinner, S., Wilson, J.C., Soos, M.A., Murgatroyd, P.R., Williams, R.M., Acerini, C.L., et al. (2004). A family with severe insulin resistance and diabetes due to a mutation in *AKT2*. Science *304*, 1325–1328.

Goodey, N.M., and Benkovic, S.J. (2008). Allosteric regulation and catalysis emerge via a common route. Nat. Chem. Biol. *4*, 474–482.

Gordon, J.C., Myers, J.B., Folta, T., Shoja, V., Health, L.S., and Onufriev, A. (2005). H^{++}: a server for estimating p*K*as and adding missing hydrogens to macromolecules. Nucleic Acids Res. *33*, W368–W371.

Guo, J., Pang, X., and Zhou, H. (2015). Two pathways mediate interdomain allosteric regulation in Pin1. Structure *23*, 237–247.

Henzler-Wildman, K., and Kern, D. (2007). Dynamic personalities of proteins. Nature *450*, 964–972.

Huang, Z., Mou, L., Shen, Q., Lu, S., Li, C., Liu, X., Wang, G., Li, S., Geng, L., Liu, Y., et al. (2014). ASD v2.0: updated content and novel features focusing on allosteric regulation. Nucleic Acids Res. *42*, D510–D516.

Humphrey, S.J., and James, D.E. (2013). Uncaging Akt. Sci. Signal. *5*, pe20.

Imai, T., Oda, K., Kovalenko, A., Hirata, F., and Kidera, A. (2009). Ligand mapping on protein surfaces by the 3D-RISM theory: toward computational fragment-based drug design. J. Am. Chem. Soc. *131*, 12430–12440.

Kumar, C.C., Diao, R., Yin, Z., Liu, Y., Samatar, A.A., Madison, V., and Xiao, L. (2001). Expression, purification, characterization and homology modeling of active Akt/PKB, a key enzyme involved in cell survival signaling. Biochim. Biophys. Acta *1526*, 257–268.

Leibiger, B., Moede, T., Uhles, S., Barker, C.J., Creveaux, M., Domin, J., Berggren, P.O., and Leibiger, I.B. (2010). Insulin-feedback via PI3K-C2α activated PKBα/Akt1 is required for glucose-stimulated insulin secretion. FASEB J. *24*, 1824–1837.

Liao, Y., and Huang, M.C. (2010). Physiological regulation of Akt activity and stability. Am. J. Transl. Res. *2*, 19–42.

Lin, K., Lin, J., Wu, W.-I., Ballard, J., Lee, B.B., Gloor, S.L., Vigers, G.P., Morales, T.H., Friedman, L.S., Skelton, N., and Brandhuber, B.J. (2012). An ATP-site on-off switch that restricts phosphatase accessibility of Akt. Sci. Signal. *5*, ra37.

Lu, S., Huang, W., Wang, Q., Shen, Q., Li, S., Nussinov, R., and Zhang, J. (2014a). The structural basis of ATP as an allosteric modulator. PLoS Comput. Biol. *10*, e1003831.

Lu, S., Li, S., and Zhang, J. (2014b). Harnessing allostery: a novel approach to drug discovery. Med. Res. Rev. *34*, 1242–1285.

Lu, S., Huang, W., and Zhang, J. (2014c). Recent computational advances in the identification of allosteric sites in proteins. Drug Discov. Today *19*, 1595–1600.

Manning, B.D., and Cantley, L.C. (2007). AKT/PKB signaling navigating downstream. Cell *129*, 1261–1274.

Nussinov, R., and Tsai, C.-J. (2013). Allostery in disease and in drug discovery. Cell *153*, 293–305.

Nussinov, R., and Tsai, C.-J. (2015). The design of covalent allosteric drugs. Annu. Rev. Pharmacol. Toxicol. *55*, 249–267.

Nussinov, R., Tsai, C.-J., Xin, F., and Radivojac, P. (2012). Allosteric post-translational modification codes. Trends Biochem. Sci. *37*, 447–455.

Sarbassov, D.D., Guertin, D.A., Ali, S.M., and Sabatin, D.M. (2005). Phosphorylation and regulation of Akt/PKB by the rictor-mTOR complex. Science *307*, 1098–1101.

Shearn, C.T., Fritz, K.S., Reigan, P., and Petersen, D.R. (2011). Modification of Akt2 by 4-hydroxynonenal inhibits insulin-dependent Akt signaling in HepG2 cells. Biochemistry *50*, 3984–3996.

Shen, A., Lupardus, P.J., Gersch, M.M., Puri, A.W., Albrow, V.E., Carcia, K.C., and Bogyo, M. (2011). Defining an allosteric circuit in the cysteine protease domain of *Clostridium difficile* toxins. Nat. Struct. Mol. Biol. *18*, 364–371.

Sindhikara, D.J., Yoshida, N., and Hirata, F. (2012). *Placevent*: an algorithm for prediction of explicit solvent atom distribution—application to HIV-1 protease and F-ATP synthase. J. Comput. Chem. *33*, 1536–1543.

Valley, C.C., Cembran, A., Perlmutter, J.D., Lewis, A.K., Labello, N.P., Gao, J., and Sachs, J.N. (2012). The methionine-aromatic motif plays a unique role in stabilizing protein structure. J. Biol. Chem. *287*, 34979–34991.

Vivanco, I., and Sawyers, C.L. (2002). The phosphatidylinositol 3-kinase AKT pathway in human cancer. Nat. Rev. Cancer *2*, 489–501.

Wang, X., Gjörloff-Wingren, A., Saxena, M., Pathan, N., Reed, J.C., and Mustelin, T. (2000). The tumor suppressor PTEN regulates T cell survival and antigen receptor signaling by acting as a phosphatidylinositol 3-phosphatase. J. Immunol. *164*, 1934–1939.

Woodgett, J.R. (2005). Recent advances in the protein kinase B signaling pathway. Curr. Opin. Cell Biol. *17*, 150–157.

Wu, W.-I., Voegtli, W.C., Sturgis, H.L., Dizon, F.P., Vigers, G.P., and Brandhuber, B.J. (2010). Crystal structure of human AKT1 with an allosteric inhibitor reveals a new mode of kinase inhibition. PLoS One *5*, e12913.

Xiao, B., Sanders, M.J., Carmena, D., Bright, N.J., Haire, L.F., Underwood, E., Patel, B.R., Heath, R.B., Walker, P.A., Hallen, S., et al. (2013). Structural basis of AMPK regulation by small molecule activators. Nat. Commun. *4*, 3017.

Zheng, J., Trafny, E.A., Knighton, D.R., Xuong, N.H., Taylor, S.S., Ten Eyck, L.F., and Sowadski, J.M. (1993). 2.2 Å refined crystal structure of the catalytic subunit of cAMP-dependent protein kinase complexed with MNATP and a peptide inhibitor. Acta Crystallogr. D Biol. Crystallogr. *49*, 362–365.

Zhou, T., Raman, M., Gao, Y., Earnest, S., Chen, Z., Machius, M., Cobb, M.H., and Goldsmith, E.J. (2004). Crystal structure of the TAO2 kinase domain: activation and specificity of a Ste20p MAP3K. Structure *12*, 1891–1900.

